

REPORT DOCUMENTATION PAGE

Form Approved
OMB No. 0704-0188

1a. F IC
1b. RESTRICTIVE MARKINGS

2a. S AD-A221 793
2b. C 1990
3. DISTRIBUTION/AVAILABILITY OF REPORT
Approved for public release; distribution is unlimited. (2)

4. PERFORMING ORGANIZATION REPORT NUMBER(S) D 8
5. MONITORING ORGANIZATION REPORT NUMBER(S)
AFOSR-TR- 90-0504

6a. NAME OF PERFORMING ORGANIZATION
Stanford University
6b. OFFICE SYMBOL (if applicable)
7a. NAME OF MONITORING ORGANIZATION
AFOSR/NA

6c. ADDRESS (City, State, and ZIP Code)
Department of Mechanical Engineering
Stanford, CA 94305
7b. ADDRESS (City, State, and ZIP Code)
Building 410, Bolling AFB DC
20332-6448

8a. NAME OF FUNDING/SPONSORING ORGANIZATION
AFOSR/NA
8b. OFFICE SYMBOL (if applicable)
9. PROCUREMENT INSTRUMENT IDENTIFICATION NUMBER
F49620-86-K-0022

8c. ADDRESS (City, State, and ZIP Code)
Building 410, Bolling AFB DC
20332-6448
10. SOURCE OF FUNDING NUMBERS
PROGRAM ELEMENT NO. 61103D PROJECT NO. 3484 TASK NO. A1 WORK UNIT ACCESSION NO.

11. TITLE (Include Security Classification)
(U) Turbulent Reacting Flows and Supersonic Combustion

12. PERSONAL AUTHOR(S)
C.T. Bowman, R.K. Hanson, M.G. Mungal and W.C. Reynolds

13a. TYPE OF REPORT
Final Technical
13b. TIME COVERED
FROM 10-1-86 TO 9-30-89
14. DATE OF REPORT (Year, Month, Day)
1990, January 15
15. PAGE COUNT
36

16. SUPPLEMENTARY NOTATION

17. COSATI CODES
FIELD GROUP SUB-GROUP
18. SUBJECT TERMS (Continue on reverse if necessary and identify by block number)
turbulent reacting flow, supersonic combustion.

19. ABSTRACT (Continue on reverse if necessary and identify by block number)
An experimental and computational investigation of supersonic combustion flows was carried out. The principal objective of the research was to gain a more fundamental understanding of mixing and chemical reaction in supersonic flows. The research effort comprised three inter-related elements: (1) an experimental study of mixing and combustion in a supersonic plane mixing layer; (2) development of laser-induced fluorescence techniques for time-resolved two-dimensional imaging of species concentration, temperature and velocity; and, (3) numerical simulations of compressible reacting flows. The specific objectives and the results of the research is summarized.
*Original contains color plates. All DTIC reproduction will be in black and white.

20. DISTRIBUTION/AVAILABILITY OF ABSTRACT
 UNCLASSIFIED/UNLIMITED SAME AS RPT DTIC USERS
21. ABSTRACT SECURITY CLASSIFICATION
Unclassified

22a. NAME OF RESPONSIBLE INDIVIDUAL
Julian M Tishkoff
22b. TELEPHONE (Include Area Code)
(202) 767-4935
22c. OFFICE SYMBOL
AFOSR/NA

TABLE OF CONTENTS

	<u>Page</u>
1.0 SUMMARY	1
2.0 INTRODUCTION	2
3.0 MIXING AND REACTION IN SUPERSONIC FLOW	3
3.1 Objectives	3
3.2 Status of the Research	3
3.2.1 Flow Facility Description.	3
3.2.2 Flow Facility Operating Range	5
3.2.3 Results on Flow Structure	5
3.2.4 Results on Flow Modeling	8
3.3 Future Work	10
4.0 SUPERSONIC FLOW DIAGNOSTICS	11
4.1 Objectives.	11
4.2 Status of the Research.	11
4.2.1 Flow Facility Development.	11
4.2.2 Laser Testing and Development	12
4.2.3 UV Imaging Camera Development	13
4.2.4 Fluorescence Spectroscopy Modelling	13
4.2.5 PLIF Imaging in Shock Tube Flows.	14
4.2.6 Temperature and Velocity Imaging in Supersonic Flows	16
4.3 Future Work	21
5.0 COMPUTER SIMULATION AND ANALYSIS	22
5.1 Objectives.	22
5.2 Status of the Research.	22
5.2.1 Linearized stability analysis for compressible mixing layers	22
5.2.2 Mixing layer simulations	24
5.2.3 Compressible isotropic turbulence.	25
5.3 Future Work	30
6.0 PUBLICATIONS AND PRESENTATIONS.	31
7.0 PERSONNEL	34
8.0 PROFESSIONAL INTERACTIONS	35
9.0 REFERENCES	36

1.0 SUMMARY

An experimental and computational investigation of supersonic combustion flows is in progress. The principal objective of the research is to gain a more fundamental understanding of mixing and chemical reaction in supersonic flows. The research effort comprises three inter-related elements: (1) an experimental study of mixing and combustion in a supersonic plane mixing layer; (2) development of laser-induced fluorescence techniques for time-resolved two-dimensional imaging of species concentration, temperature and velocity; and, (3) numerical simulations of compressible reacting flows. The specific objectives and the status of the research of each of these program elements is summarized in this report.

Accession For	
NTIS CRA&I	<input checked="" type="checkbox"/>
DTIC TAB	<input type="checkbox"/>
Unannounced	<input type="checkbox"/>
Justification	
By	
Distribution /	
Availability Codes	
Dist	Avail and/or Special
A-1	



2.0 INTRODUCTION

Air-breathing propulsion systems offer the potential of higher performance than conventional rocket engines for hypersonic flight. To realize this potential, new combustor design concepts are required. In particular, in order to minimize losses associated with strong shock waves and high combustor inlet temperatures, it is desirable to maintain high flow velocities in the combustion chamber. This design concept leads to a new class of propulsion devices where combustion takes place in supersonic flow.

Combustion in supersonic flow is fundamentally different from combustion in the subsonic flow regime employed in all currently operating aircraft engines. Many of the design approaches developed over the years for subsonic combustors, e.g. ignition and flame stabilization techniques, are not applicable to supersonic combustion devices, and the current understanding of the fundamental aspects of supersonic combustion is inadequate to support the development of these devices (Defense Science Board Report, 1988).

Recent advances in diagnostic capabilities and significant improvements in our ability to compute such flows offer new opportunities to obtain the needed fundamental understanding of compressible turbulent reacting flows. To achieve this understanding, a closely coordinated experimental and computational program which utilizes state-of-the-art experimental techniques and computational methods is needed. We have been engaged in such an effort over the past 36 months with support from the Air Force Office of Scientific Research.

The principal objective of the research is to gain a more fundamental understanding of the flow physics and chemistry interactions in compressible turbulent reacting flows. The project comprises three interrelated efforts: (1) an experimental study of mixing and combustion in supersonic flows, (2) development of laser-induced fluorescence techniques for time-resolved multi-dimensional imaging of species concentration, temperature, and velocity in supersonic flows, and (3) simulation and modeling of supersonic flows with mixing and chemical reaction. A close coupling among these efforts is maintained in order to maximize our understanding of supersonic turbulent reacting flows, with emphasis on supersonic combustion. The specific objectives and status of the research of each of the program elements is described below.

3.0 MIXING AND REACTION IN SUPERSONIC FLOW

3.1 Objectives

A primary goal of our research is to understand the effects of compressibility upon mixing and combustion in a fundamental way. Hence, it is desirable to study as simple a flow as possible so that compressibility effects can be quantified. With this objective in mind, the two-dimensional supersonic mixing layer was chosen for initial study. Other candidate fundamental flows, namely the jet in coflow or the jet in crossflow, while simpler to implement experimentally, were considered too complicated to interpret in a fundamental way.

An important benefit of the mixing layer is that a single parameter, the convective Mach number (Bogdanoff, 1983; Papamoschou and Roshko, 1986), has been proposed for quantifying the effects of compressibility on the development of the layer. Furthermore, there exists a considerable body of knowledge about mixing layers in the incompressible regime that can be used for comparison with the compressible case, thus providing clear indications of the effects of compressibility. The mixing layer also lends itself well to laser-based imaging techniques, and it is well-suited to attack by numerical computations.

An additional benefit of the two-dimensional mixing layer is that the flow allows for systematic study of mixing enhancement techniques such as freestream forcing, interaction with shock waves or expansion fans, and the use of wavy walls and streamwise curvature to generate additional instabilities and hence improve mixing.

3.2 Status of the Research

A primary requirement of an experimental facility for investigation of supersonic combustion flows is achievement of realistic flow conditions at a scale that is sufficiently large to yield meaningful results but not so large as to become unmanageable by university standards. This led us to design and construct a large facility capable of producing compressible flow conditions for mixing and combustion studies. In the following sections, the flow facility is described and results from initial experiments on compressible mixing layers are presented.

3.2.1 Flow Facility Description

A two-stream, two-dimensional, supersonic, mixing layer facility has been designed and constructed, see Fig. 1. The primary goals in designing the facility were attainment of significant convective Mach numbers and attainment of fast combustion. Details of the

design are discussed in papers 22 through 24 by Clemens et al., listed in Section 6.0, and only a brief overview will be provided here.

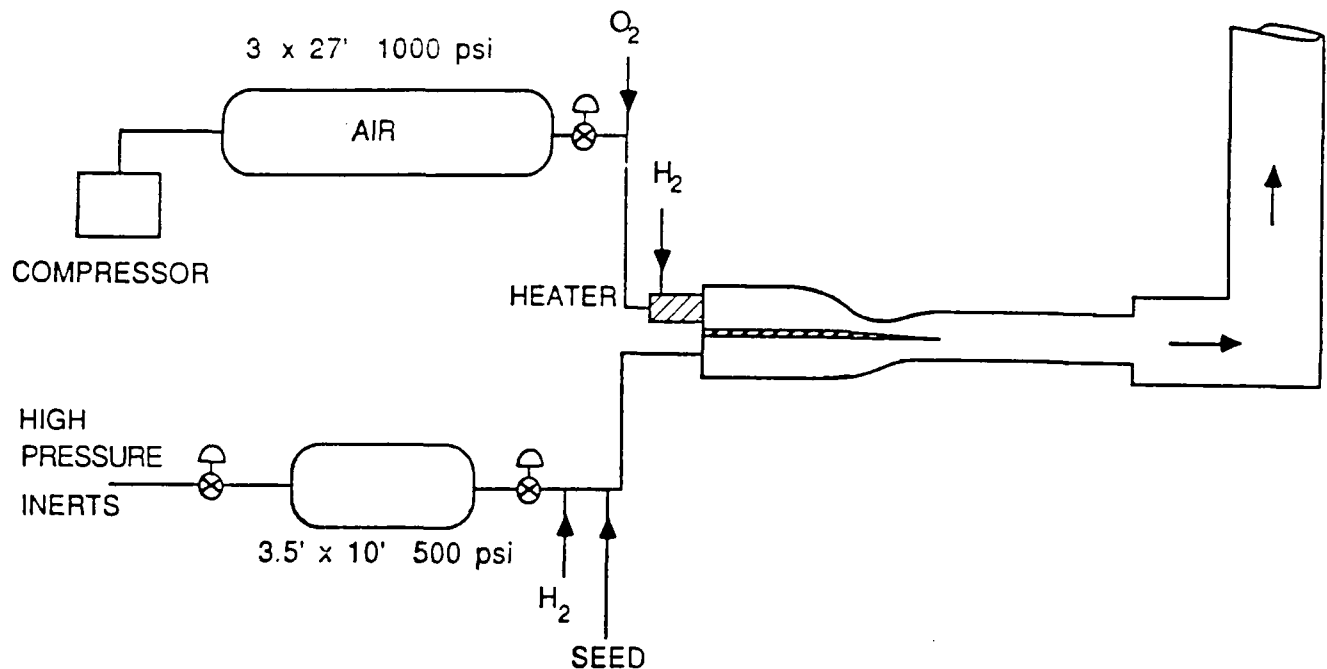


Figure 1. Schematic Diagram of the Stanford Supersonic Shear Flow Facility.

The high-speed stream consists of a Mach 2 vitiated air stream in a 10 cm x 2.5 cm exit area, with mass flow rates varying from 2.8 kg/s at 300K stagnation temperature to 1.0 kg/s at 2000K. These elevated stagnation temperatures are produced by a Marquardt SUE (SUdden Expansion) burner using hydrogen as a fuel. The low-speed stream is nominally Mach 1 in a 10 cm x 3 cm exit area with a mass flow rate of 1.4 kg/s at 300K stagnation temperature. The low-speed stream can be either air or inert gas (with possible tracer gas) for non-reacting mixing experiments, or a mixture of inert gas and hydrogen for reacting flow experiments. The test section operates nominally at atmospheric pressure and provision is made for optical access through all four sides. The first 40 cm of the test section is available for obtaining measurements. The facility has been designed for a maximum possible high-speed Mach number of 2.5.

The high-speed air is supplied from a 1000 psi pressure air vessel, while the low-speed stream is drawn from a 500 psi pressure vessel. Maximum run time, limited by the stored gas supply, is approximately 100 seconds. The facility has been designed to handle maximum stagnation temperatures of 2200K, the maximum capability of the SUE burner. On exiting the test section, the exhaust gas enters a supersonic diffuser before it is dumped into an exhaust duct. The flow is cooled by use of high pressure water sprays as it exits through the exhaust stack. Figure 2a is a photograph of the facility showing the control

panel, inlet flow piping and computer-controlled flow regulating valves together with the flow rig. Figure 2b shows a closeup of the plenum, nozzle and test section with the side wall removed.

3.2.2 Flow Facility Operating Range

Figure 3 shows a range of achievable convective Mach numbers, M_c , for the case of $M_2 = 1.0$, $T_{02} = 300\text{K}$, nitrogen, $M_1 = 2.0$, $T_{01} = 300 - 2000\text{K}$, vitiated air. A significant variation of convective Mach numbers can be obtained simply by changing the high-speed stagnation temperature with all other parameters remaining fixed. The density ratio changes significantly with changes in stagnation temperature, but this is not considered an important issue, since comparisons usually are made with incompressible flows for which the density and velocity ratios are the same as the compressible case. An alternative approach to obtaining significant convective Mach numbers is by simply decreasing the low-speed Mach number for fixed high-speed Mach number. This approach has been followed for our first sets of experiments until the burner becomes fully operational.

For the reacting flow experiments, hydrogen, up to 20% by volume, corresponding to a stoichiometric overall fuel/air ratio, will be added to an inert low-speed stream. The high-speed stream, consisting of vitiated air, will be run at a stagnation temperature of about 2000K, in order to ensure ignition in the test section. The high-speed Mach number will be lowered, possibly to as low as 1.6, in order to maintain a high static temperature in the test section, with a still significant convective Mach number of about 0.8. We have developed a simplified model of the supersonic reacting mixing layer to allow prediction of the expected ignition times and Damköhler numbers.

In summary, we have an operational supersonic facility that spans the range from incompressible to compressible flow regimes. By changing the high-speed stagnation temperature from 300K to 1000K or by decreasing the low-speed Mach number, we can obtain convective Mach numbers in the range of 0.3 to 0.8. Higher convective Mach numbers can be obtained by slowing the low-speed stream or by using a heavy gas on the low-speed side. In combustion studies, the high-speed stagnation temperature will be increased to 2000K while flowing a mixture of hydrogen and nitrogen in the low-speed stream.

3.2.3 Results on Flow Structure

A series of experiments aimed at determining the structure of the mixing layer for a low and a high convective Mach number have been performed. For these experiments both streams are run at room temperature stagnation conditions. In the low convective Mach

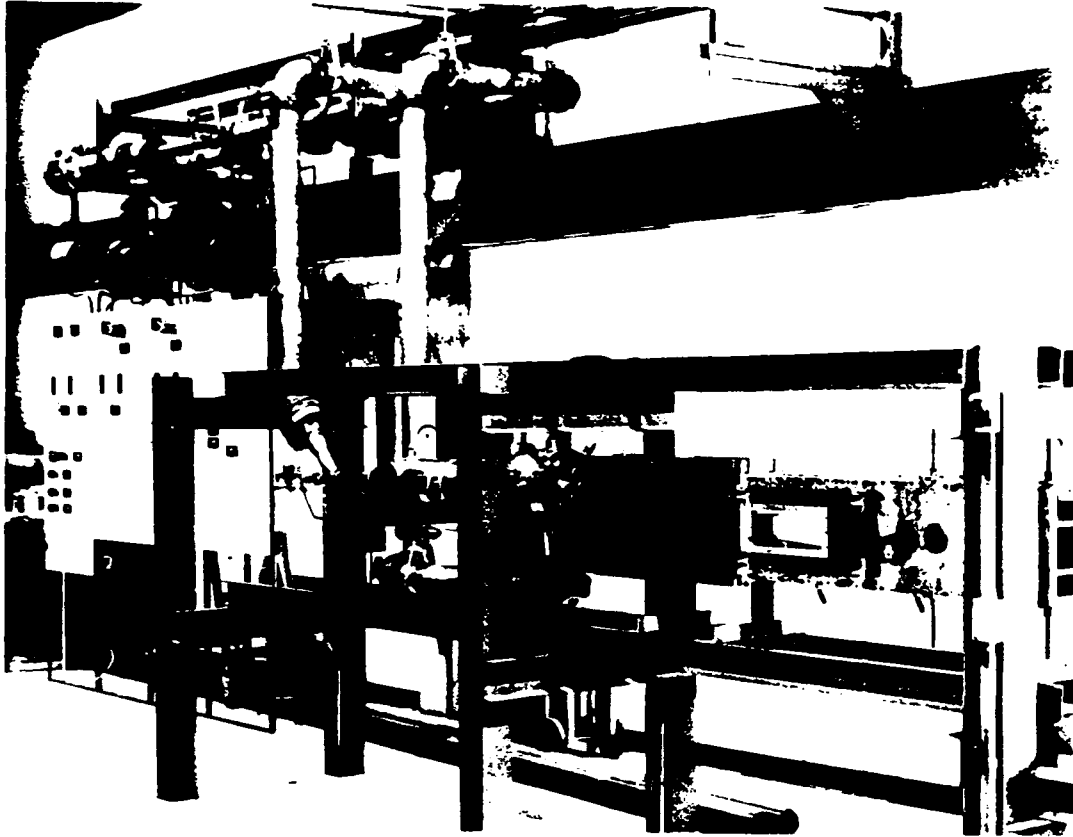


Figure 2a. Photograph of the Stanford Supersonic Shear Flow Facility.

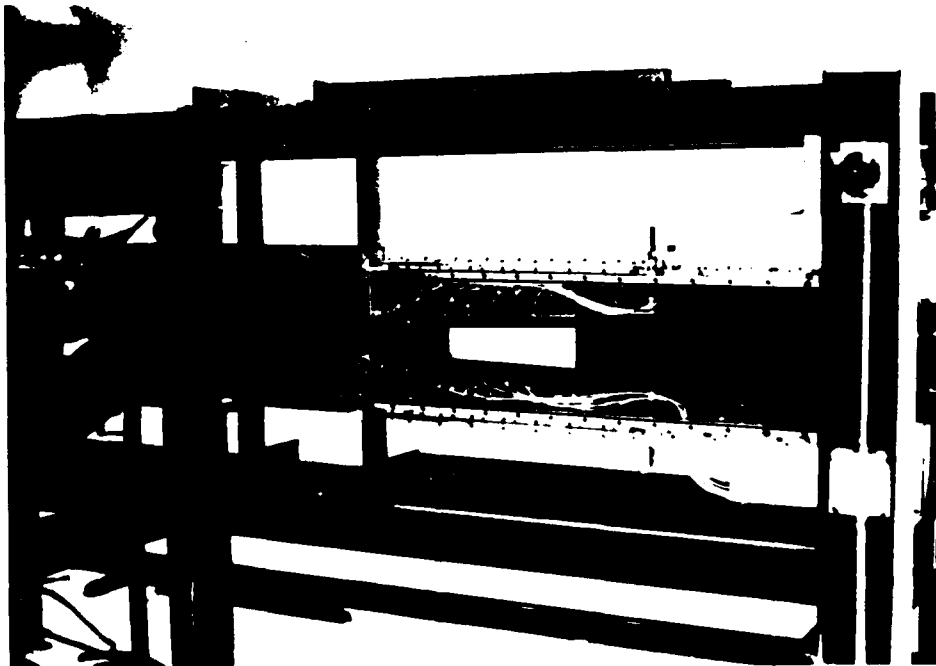


Figure 2b. Photograph of the Plenum, Nozzle and Test Section.

$M_1 = 2.0, M_2 = 1.0, T_{02} = 300 \text{ K}, T_2 = 250 \text{ K}, U_2 = 322 \text{ m/sec}, \rho_2 = 1.3 \text{ kg/m}^3, \gamma_2 = 1.4$

\dot{M}_1 (kg/sec)	T_{01} (K)	T_1 (K)	γ_1 (stagnation)	U_1 (m/sec)	ρ_1 (kg/m ³)	M_{c1}	δ/x	Re./cm (x10 ⁻⁵)
2.6	300	167	1.40	517	2.0	.34	.064	3.4
1.8	600	349	1.36	737	.98	.60	.090	2.1
1.5	900	542	1.33	918	.63	.77	.045	1.4
1.2	1200	740	1.31	1080	.45	.89	.054	1.1
1.1	1500	938	1.30	1227	.35	.98	.061	.86
.94	1800	1154	1.28	1375	.27	1.0	.069	.71
.84	2100	1381	1.26	1527	.22	1.1	.077	.60

Figure 3. Run Matrix.

number experiment, $M_1 = 1.5$ and $M_2 = 0.7$, yielding $M_c = 0.3$ while for the high convective Mach number experiment, $M_1 = 2.0$ and $M_2 = 0.6$, yielding $M_c = 0.6$. The structural aspects of the mixing layer are investigated by use of planar laser Mie scattering. In this technique, alcohol vapor seeded in the low-speed stream condenses to form fine alcohol droplets on contact with the cold high-speed stream. A laser sheet interrogates the resulting droplet cloud, which effectively marks the mixing region. Images of the side, plan and end views are used to infer the flow structure.

Fig. 4 shows the plan view for the low and high convective Mach number cases. For the low M_c case, where the flow should behave incompressibly, the structure is generally two-dimensional, while for the high case there is considerably more three dimensionality present. Interestingly, these results are in accord with the numerical simulation results presented in Section 5. Further details of these experiments can be found in papers 22 through 24 by Clemens et al. listed in Section 6.0. It appears then that there is a definite change in the flow structure as compressibility increases. In our future studies, using the PLIF approaches described in Section 4, we plan to measure the probability density function of mixture fraction as a function of increasing compressibility. These results will be important to modelling efforts and also to determining the overall stoichiometry of reactions under compressible conditions.

3.2.4 Results on Reacting Flow Modeling

A simplified model for compressible, reacting mixing layers has been developed. Fig. 5. The model is similar to the Broadwell-Breidenthal-Mungal model (see Broadwell & Breidenthal, 1982 and Broadwell & Mungal, 1988) but allows for the inclusion of a complex chemistry model, which is necessary for predicting the effects of finite-rate chemistry. Combustion in the mixing layer is modeled as occurring in two modes: a strained, diffusion flame mode and a well-mixed mode. The strained, diffusion flame combustion mode is modeled using the results of one-dimensional, strained, laminar diffusion flame calculations, which included full chemical kinetics. The premixed combustion mode is modeled as a homogeneous, constant pressure reactor with mass entrainment. The model contains only one free parameter that specifies the fraction of entrained fluid which flows into each reactor. The model was used to calculate the ignition length of a compressible mixing layer with supersonic, high temperature air and sonic, ambient temperature hydrogen as the free stream reactants. The predicted ignition length compared favorably with the experimentally measured value (Burrows and Kurkov, 1973). The model was also used to investigate the sensitivity of ignition length and extent of reaction of a supersonic mixing layer to fuel stream hydrogen concentration, air stream temperature and convective Mach number. Both the ignition length and the extent of reaction were found to be sensitive to all of these

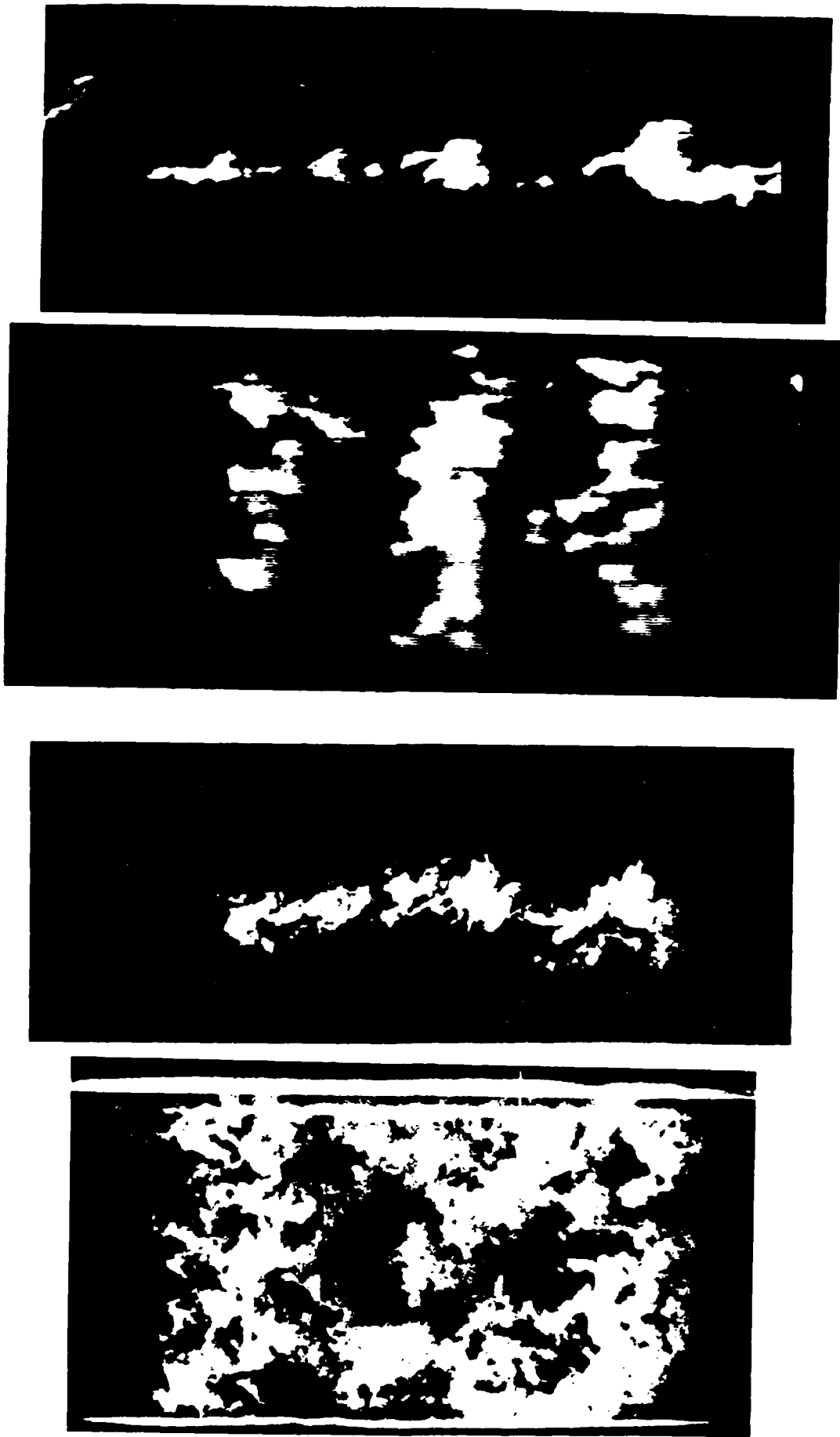


Figure 4. Plan and Side Views of Planar Mie Scattering Images of Supersonic Mixing Layer. Top Photos $M_c = 0.3$. Bottom Photos $M_c = 0.6$. Note Evidence of Two-Dimensionality for Low M_c Case.

variables. Further details of the model formulation and results are described in paper 25 by Miller et al. listed in Section 6.0.

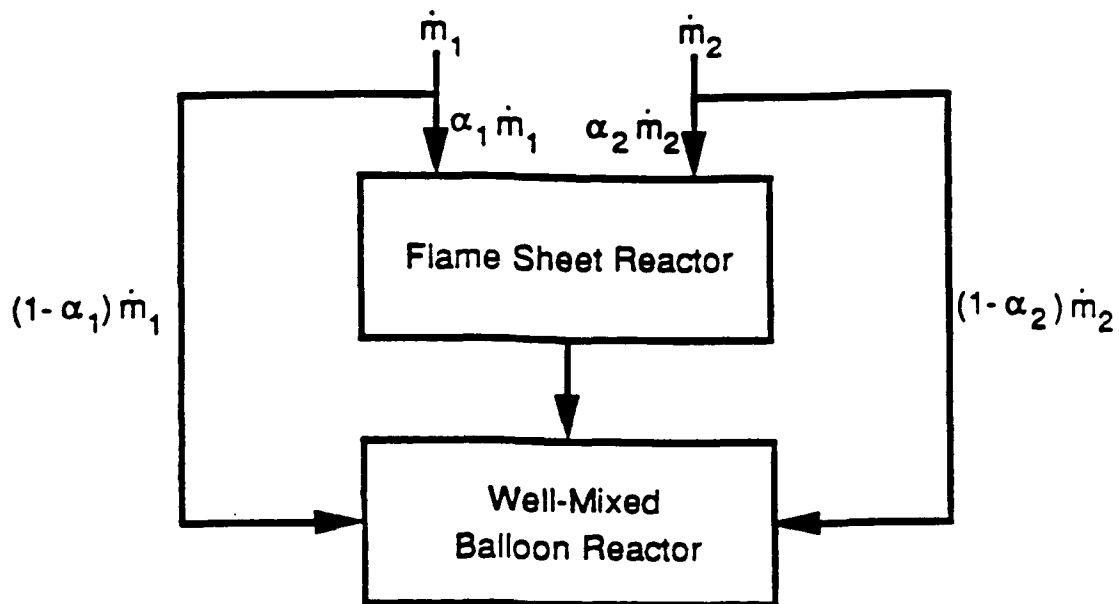


Figure 5. Flow reactor schematic of the model.

3.3 Future Work

During the next three years of the program we plan to continue the work discussed above and to initiate new work as described in our renewal proposal. This work includes:

- Complete full structural description of the compressible mixing layer
- Using PLIF approaches, measure the probability density function of mixture fraction under compressible conditions
- Initiate compressible burning studies to determine ignition limits
- Use PLIF to determine overall combustion efficiency.
- Explore effects of Damköhler number upon chemical reaction in the compressible mixing layer.

4.0 SUPERSONIC FLOW DIAGNOSTICS

4.1 Objectives

This aspect of the research is aimed at developing flowfield imaging diagnostics based on Planar Laser-Induced Fluorescence (PLIF). Flow parameters of interest include species concentrations (or mole fraction), temperature, velocity and pressure. Particular emphasis is placed on imaging molecular oxygen (O_2) and nitric oxide (NO), since these species are naturally present in nearly all supersonic flows of practical interest.

4.2 Status of the Research

Work over the period of this program has been in six areas: (1) flow facility development; (2) laser testing and development; (3) uv imaging camera development; (4) fluorescence spectroscopy modelling; (5) PLIF imaging in shock tube flows; and (6) temperature and velocity imaging in supersonic flows.

4.2.1 Flow Facility Development

In order to provide user-friendly test environments for developing PLIF imaging diagnostics for supersonic flows, we elected to build three new flow facilities. The first facility, already in use, is a small-scale, electrically heated (to 1000 K) supersonic jet. The jet is operated continuously, usually in an underexpanded flow mode with a background pressure of 5-50 torr. This facility provides convenient access to a wide range of gaseous mixtures and flow conditions, including Mach numbers up to about 7. The disadvantages of the facility are that the stagnation enthalpy is somewhat limited, relative to values expected in future scramjets, and that the flowfield is quite small. These limitations will be removed with the completion of the two larger flow facilities discussed below. In the meantime, the small-scale facility has allowed experimentation to proceed on candidate PLIF imaging concepts, and results from these experiments have already been presented at meetings and in recently submitted publications (see list in Section 6.0).

A second facility, also completed, utilizes plasma heating of the test gases to achieve high stagnation enthalpies prior to expansion to supersonic conditions. This facility features a 75 kW RF power supply which drives a plasma torch operable at pressures up to about 4 atmospheres and equilibrium air temperatures of about 5000 K. The torch serves as the stagnation chamber for a contoured nozzle and downstream supersonic flow test section. The facility is connected to a vacuum pumping station of sufficient capacity to allow continuous operation at background pressures down to 50 torr, mass flow rates of a few

gm/sec, and expanded flow velocities up to about 4 km/sec. The nozzle throat diameter is 8 mm. The facility is fully assembled and is currently in use in research on diagnostics for high-speed nonequilibrium air flows.

The final facility, now nearing completion, is a shock tunnel. A shock tunnel is the optimum choice for producing very high stagnation enthalpies in a clean flow environment and at modest expense. The disadvantage is that it is a pulsed flow facility. At present we have completed construction of the shock tube portion of the system, and preliminary imaging experiments of shock-heated O₂ and NO have been carried out successfully (see Sec. 4.2.5). Finally, fabrication of the shock tunnel addition to the tube has been initiated, and we expect to have the first-generation nozzle and hypersonic flow test section functional during the coming year.

4.2.2 Laser Testing and Development

During the first year of this program, we acquired a tunable narrow-linewidth excimer laser which offers high potential for various PLIF imaging strategies. Unfortunately, as we began to use the laser, we identified certain performance limitations, especially when operating at the argon fluoride wavelength of 193 nm. During the second year we modified the laser to improve its performance, particularly as regards linewidth, energy/pulse, stability and line-locking ratio. Finally, during this past year we have built an on-line laser monitor, comprised of a linear CCD array and monochromator, which allows convenient alignment of the excimer to provide optimum output characteristics and continuous recording of locking efficiency.

A related laser development activity has been our assembly of a Raman shifter suitable for use with an argon fluoride excimer laser at 193 nm. The standard commercial Raman shifter available from Lambda-Physik is designed for use at longer wavelengths, thereby necessitating some modifications. These modifications are now complete and work has been initiated to establish PLIF strategies (for O₂, OH and NO) at both down-shifted and up-shifted frequencies from the primary 193 nm photon energy.

Finally, in the past 18 months we implemented an important improvement in our excimer-pumped dye laser system. Specifically, a newly developed frequency-doubling crystal, beta-barium-borate, was installed in the doubling assembly of our Lambda-Physik 2002E dye laser. The new system affords a substantial increase in the pulse energy available at UV wavelengths; for example, in the important wavelength region 225-230 nm needed for (0,0) A ← X excitation of NO, the pulse energy was increased to about 10 mJ from its previous value of about 1 mJ. This factor of ten represents a critical performance improvement for PLIF imaging at low light levels.

4.2.3 UV Imaging Camera Development

A critical feature of imaging O_2 and NO is the fact that the fluorescence is largely in the ultraviolet region of the spectrum. This leads to a requirement that the photocathode of the camera intensifier be sensitive at these wavelengths. The low light levels expected lead to a further requirement on the size of the camera pixels, namely that they be large enough to capture enough photons to provide the needed signal-to-noise ratio. These combined requirements have led to a design for an advanced, sensitive uv imaging system based on a Reticon photodiode array with an attached fiberoptic bundle. A single microchannel plate intensifier (S-20 photocathode) is employed with the camera stub butted directly to the phosphor output of the intensifier. The entire system has been assembled and is now operational using interchangeable 128×128 or 256×256 pixel arrays. This camera has two additional features: (1) it can be operated at variable framing rate, up to 400 full frames/sec for the $(128)^2$ array; and (2) it can be used as a single-shot, frame-on-demand camera for imaging in pulsed flow facilities. The latter characteristic has proven to be critical for our PLIF imaging in a shock tube (see Sec. 4.2.5).

During the past two years we have also assembled the first intensified video-compatible camera system for PLIF imaging. This system, based on a new low-noise (240×512 pixel) Amperex CCD camera, is fully compatible with a variety of commercially available frame grabbers that are hosted directly in a PC. We have also generated a variety of necessary image processing software (not available commercially) for use with the camera system. Finally, during the past few months we have begun work on a next-generation video-compatible camera based on a new Thomson CCD array which features larger pixels and greater potential dynamic range. Our current effort is aimed at using this camera as the basis of a multiple-camera imaging system, since it is clear that many of the promising supersonic flow diagnostics concepts will require multiple camera recording.

4.2.4 Fluorescence Spectroscopy Modelling

Considerable work has been done to develop detailed spectroscopic models for O_2 , NO and OH. Such models contain capability to calculate absorption spectra (as a function of temperature and pressure) as well as the two primary forms of fluorescence: fluorescence spectra (for a specified excitation wavelength) and excitation spectra. These various models are needed for evaluating potential PLIF diagnostic schemes and for interpreting laboratory imaging data sets. Furthermore, the use of such models reveals fundamental parameters, such as electronic quench rates, which require further measurements to enable quantitative use of the diagnostic scheme selected.

A particularly important development during the past 18 months was our realization

that tunable excimer laser radiation at 193 nm may provide a significant improvement in signal-to-noise ratio for imaging of NO. Nitric oxide (NO) is a leading candidate for PLIF imaging in supersonic flows, since it is naturally present in many high temperature air systems and is easily seeded into many other supersonic flows. The currently accepted strategy for exciting NO is to pump γ -band transitions ($A \leftarrow X$) near 225 nm. This requires use of frequency mixing techniques, resulting in relatively low laser energy/pulse. Very recently, however, colleagues in Germany (P. Andresen, 1988) pointed out that the oscillator strength for absorption and emission is much stronger for ϵ -band ($D \leftarrow X$) transitions, and that energies of those transitions are well-matched to the highly energetic (over 100 mJ/pulse) argon fluoride laser at 193 nm. (See Fig. 6 for a schematic energy level diagram.) For example, our current tunable narrow-linewidth argon fluoride laser has a pulse energy of about 120 mJ and is tunable over the range 192.8-193.8 nm, which overlaps a number of isolated NO absorption lines. Following Andresen's suggestion, we modified our NO spectroscopic model and have begun to examine some of the possibilities associated with use of strong laser excitation at 193 nm. Sample calculations, aimed at providing a comparison between excitation in the γ and ϵ bands, are shown in Fig. 7. Here, all the parameters in the fluorescence equation have been fixed at reasonable values; in most cases these parameters are common to the two excitation strategies and thus effectively cancel on the relative scale of Fig. 7. For both excitation strategies, optimum rotational transitions were selected at each temperature of the plot. The clear conclusion from this graph is that at temperatures above about 600 K the new strategy offers important potential for improved SNR or lower detection limits. For example, at 1200 K, the new strategy should yield an order of magnitude increase in signal over the present method. It may also be noted that the experimental arrangement is much simpler with the new strategy, since a frequency-doubled dye laser is not required. Furthermore, the new strategy may offer opportunities for simultaneous imaging of NO and O₂, since O₂ is also easily excited at these wavelengths. At present, this new $D \leftarrow X$ (and $C \leftarrow X$) strategy is being investigated both in flame and shock tube experiments.

4.2.5 PLIF Imaging in Shock Tube Flows

Nonequilibrium hypersonic flows, relevant to current research on scramjets, pose new measurement problems for experimentalists. For example, experiments are often conducted in pulsed flow facilities in which the available measurement time is quite limited, thereby putting a premium on the ability to acquire complete data sets in very short times. In addition, many flows of interest exhibit a high degree of nonequilibrium, thereby requiring experimental methods sensitive to such nonequilibrium effects. PLIF has high potential for dealing with both of these critical problems, in that the data provide population densities in

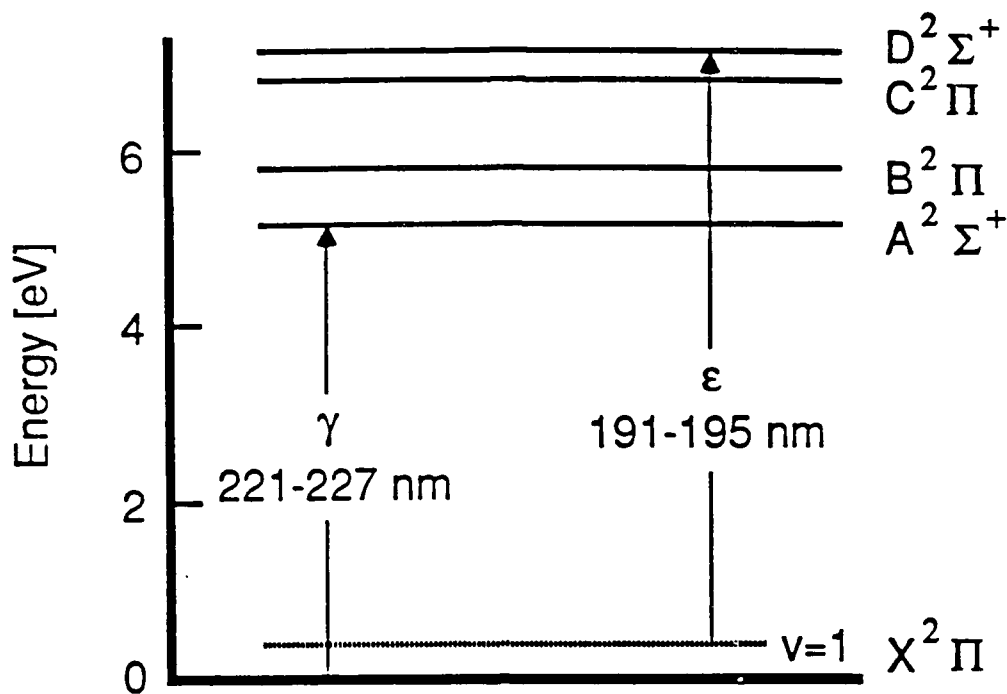


Figure 6. Energy level diagram of nitric oxide (NO). Two LIF excitation schemes, γ band ($A^2\Sigma^+ \leftarrow X^2\Pi$) excitation from the ground vibrational state and ϵ band ($D^2\Sigma^+ \leftarrow X^2\Pi$) excitation from $v = 1$, are illustrated.

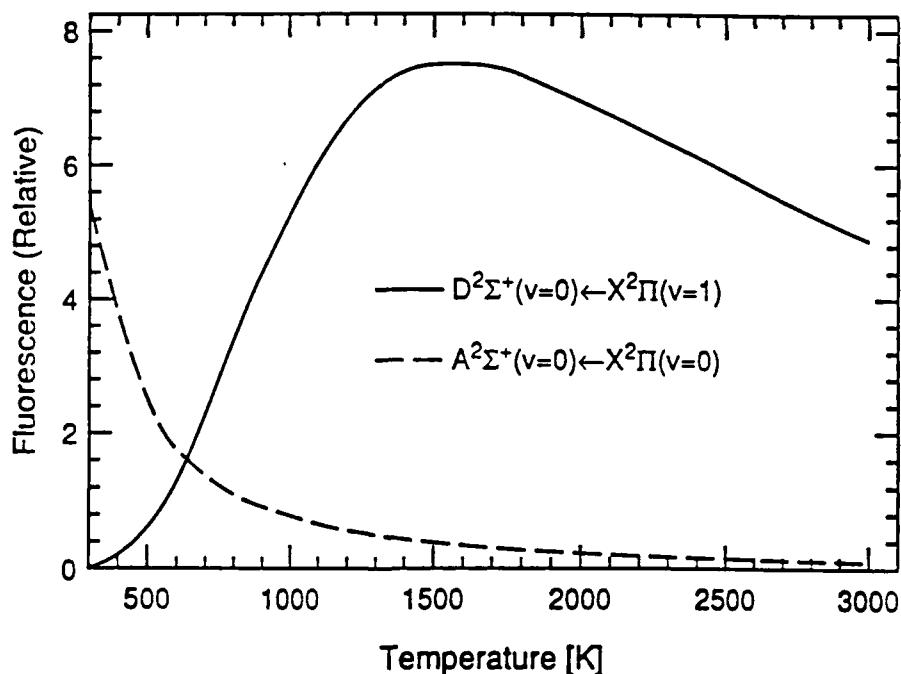


Figure 7. Comparison of the fluorescence produced by γ and ϵ band excitation of NO. We have assumed the ArF laser's spectral intensity is 7.5 times that of a typical frequency-extended dye laser system. The calculations were performed for a constant mole fraction of NO, and at each temperature, we chose the rotational transition which maximized the fluorescence.

specific quantum states of the species probed at a very large number of flowfield locations. During the past two years we have initiated research which addresses some of the problems inherent in extending PLIF to transient hypersonic flows, and these experiments are now beginning to yield important results.

Most of the experiments have been conducted in a standard pressure-driven shock tube and have emphasized measurements of nitric oxide (NO). This species is attractive owing to its presence in many combustion and high temperature air flows of interest. An initial problem, now resolved, concerned synchronization of the laser pulse and intensified camera gate with the shock wave location. This now can be done with an uncertainty of less than one microsecond, or equivalently a few millimeters of shock location. In addition, a new square shock tube, designed to facilitate imaging experiments, has been assembled and put into routine operation. Research in the past few months is illustrated by Fig. 8 which shows a PLIF image for shock-induced supersonic flow over a wedge. Of particular interest is the observation of a curved shock wave, which is a result of significant vibrational equilibrium. Significant aspects of current research involve selection of optimum laser wavelengths for excitation of NO and development of a suitable model describing the finite spatial resolution of the imaging system. Details of this work are available in papers 18 and 20 by McMillin et al. listed in Section 6.0.

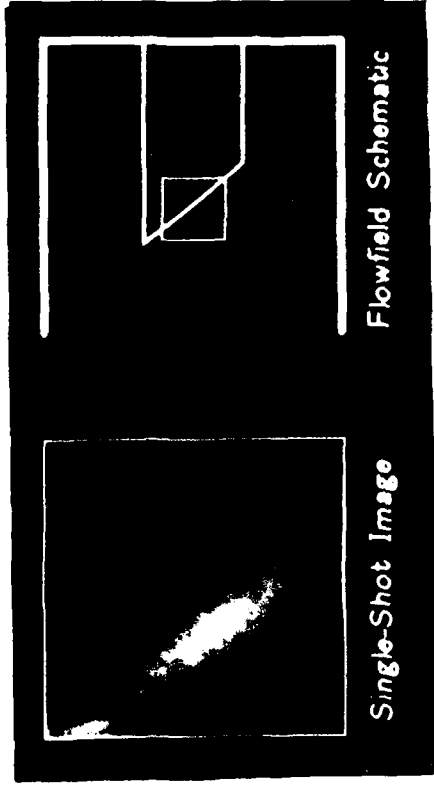
To our knowledge, this work represents the first application of PLIF to hypersonic flows, flows with vibrational nonequilibrium, and to pulsed flow facilities. The potential of PLIF for fundamental and applied studies of such flows is clear, and the results have already generated considerable interest in the hypersonic flow community.

4.2.6 Temperature and Velocity Imaging in Supersonic Flows

In supersonic, compressible flows parameters of particular importance include temperature and velocity, and new methods of probing these quantities nonintrusively are urgently needed. PLIF schemes are especially attractive owing to the relatively high signal levels which can be achieved and the potential ability to acquire 2-d (and eventually 3-d) data sets in a single laser shot. Over about the past two years we have utilized a continuous flow, supersonic underexpanded jet facility to investigate PLIF concepts in supersonic flows. Recently, we have made particular progress on imaging temperature and velocity, and these results are summarized here.

With regard to temperature, good results have been obtained with two methods, referred to as the "single line" and "two-line" concepts. In both cases the measured signal (at each flowfield point or pixel) essentially reflects the population density in a specific quantum state of the species probed. With the single-line approach, the PLIF signal is generated by

Vibrational Nonequilibrium in
Supersonic Flow over a Wedge



0.5% Nitric Oxide in Nitrogen

$M_\infty = 1.6$, $T_\infty = 1103$ K, $P_\infty = 0.47$ atm

- Images reveal shock wave structure and record nonequilibrium flowfield phenomena
- Technique permits species and quantum state-specific analysis
- Applicable to high enthalpy, hypersonic flow facilities (shock tunnels, arc jets)

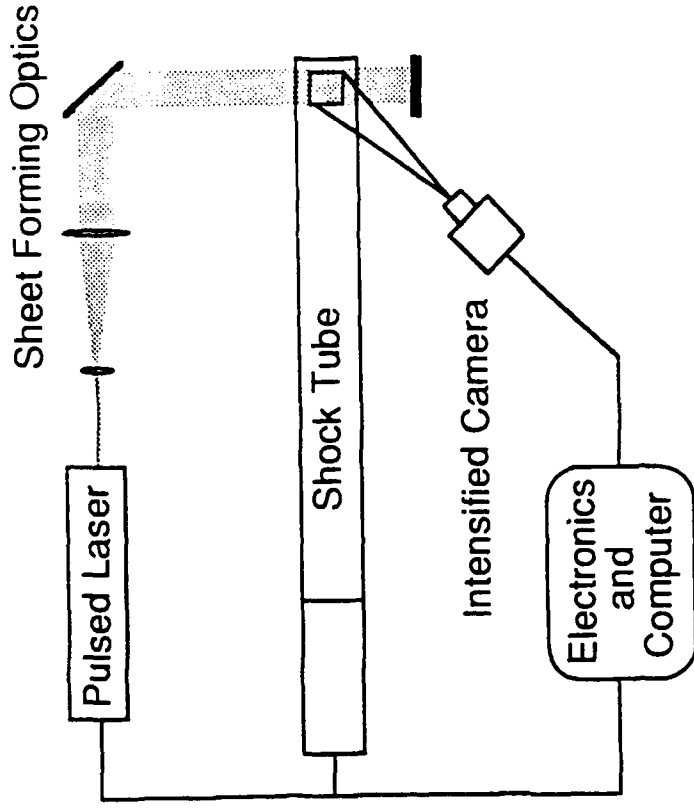


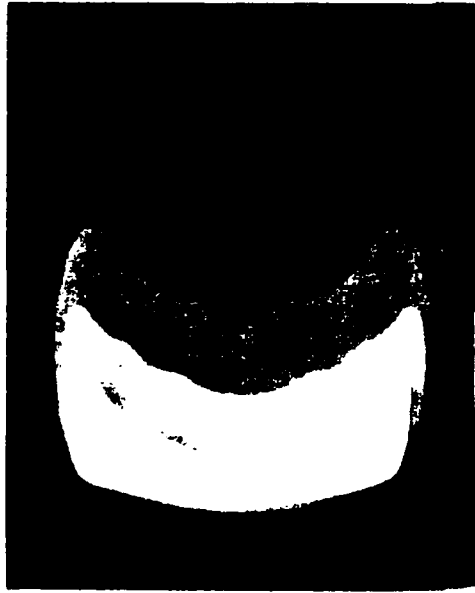
Figure 8. PLIF Imaging Used to Probe Nonequilibrium in Pulsed Supersonic Flows.

Hanson/Stanford

exciting only a single absorption line, using a single laser. In the two-line approach, two absorption lines are excited sequentially (with two lasers) and used to generate two separate PLIF images. In any case, the signal is proportional to both the mole fraction of the species and to the temperature-dependent Boltzmann fraction in the absorbing state. When the mole fraction is constant (i.e., a nonreacting flow), the PLIF signal variations across the flow essentially reflect temperature variations, and the single-line concept can be used (together with a simple calibration) to image temperature. For reacting flows (i.e., varying mole fractions), the two-line approach is necessary; in this case the ratio of the two signals is utilized, since that removes the dependence on mole fraction.

Our research has been concerned with exploring these ideas in flows containing NO, O₂ and OH. A sample result for NO in a strongly underexpanded jet ($M = 7$ at the Mach disk) is shown in Fig. 9. Although work remains to optimize the measurement strategy and to evaluate the absolute accuracy, the good signal levels obtained are a positive indication of the progress being made to develop this new measurement concept. To our knowledge, these are the first 2-d temperature images obtained by LIF in supersonic flows. Details of this work are available in paper 21 by Lee et al. listed in Sec. 6.0.

Efforts to image velocity have been based on the Doppler effect, which has the effect of shifting the relative frequencies of an illumination laser and a molecular absorption line when the gas is moving relative to the direction of laser illumination. When the laser is slightly nonresonant with the absorption line, changes in velocity (in the laser direction) result in a modulation of the light absorbed and, hence, in the quantity of fluorescence emitted. Of course other flowfield variations, such as density, can also affect the fluorescence signal, and so much of our research has been aimed at finding strategies which allow simple relationships between fluorescence signal and velocity. At present, our preferred strategy involves use of forward and counterpropagating laser beams, so that two PLIF images are generated with each laser pulse. This generates two PLIF signals at each flowfield point, and processing of these signals to find the relative change in the signal with laser direction, leads directly to the velocity component. An example of this work, using NO seeded at low levels in a supersonic underexpanded jet, is shown in Fig. 10. As shown in the right-hand panel, agreement between the measured and calculated velocities is quite good. Although this work is still in a preliminary stage, the results obtained are extremely promising in terms of developing a nonintrusive scheme for imaging velocity. Such a method will be especially important in future hypersonic flow research where traditional LDV methods are not feasible. For details, see the papers by Paul et al. listed in Section 6.0.



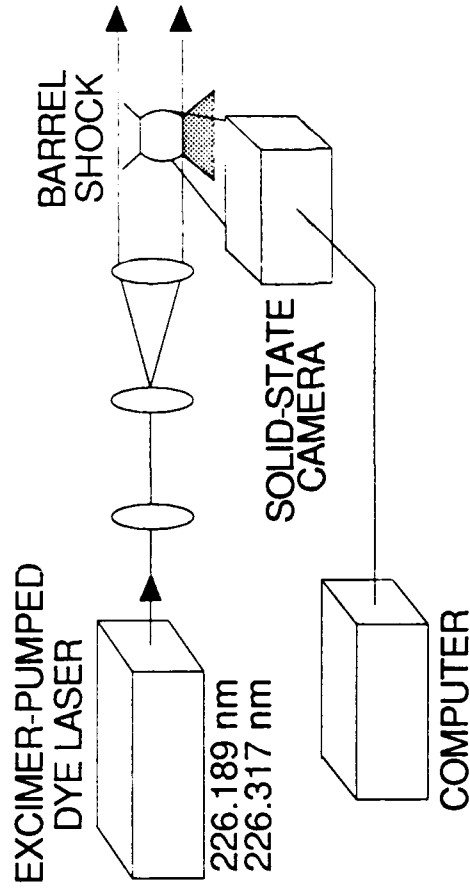
32K 35K 40K 50K 75K 150K 250K

PLIF IMAGE OF TEMPERATURE

- Technique applicable to several species, including NO, OH and O₂

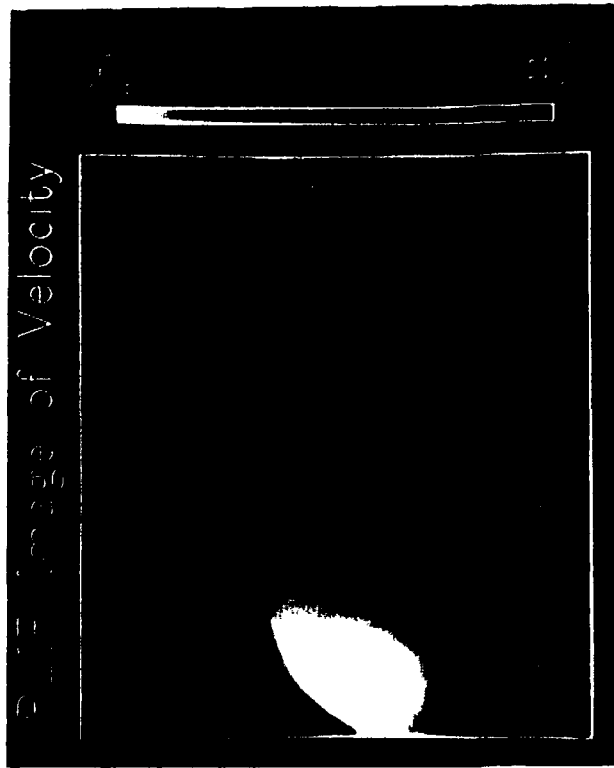
Future Research

- Perform single-shot imaging
- Simultaneous temperature and velocity imaging



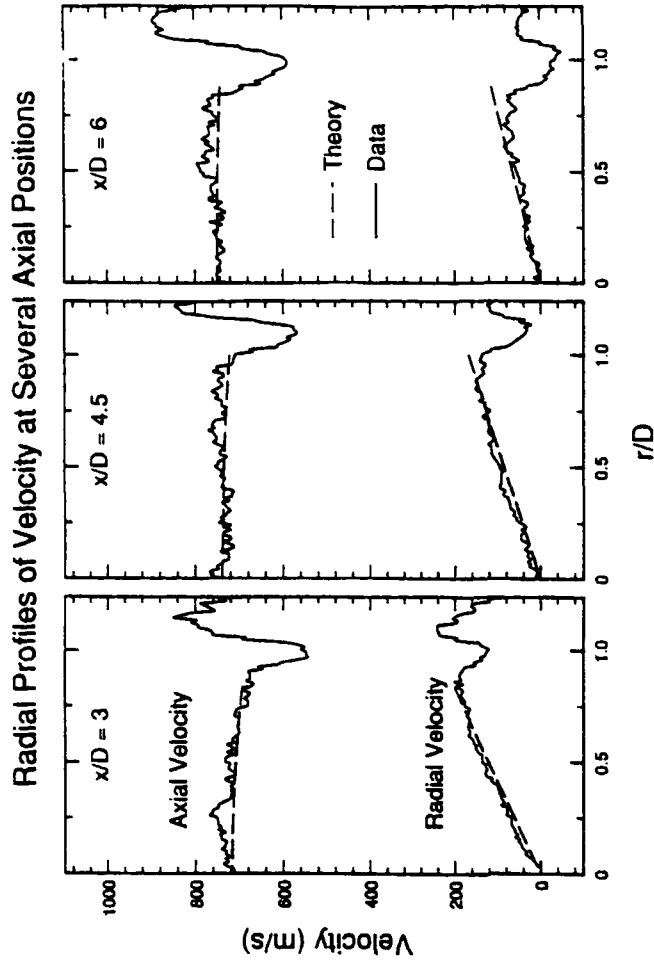
EXPERIMENTAL SCHEMATIC

Figure 9. First 2-D Temperature Measurements Made in Supersonic Flows.



One-component velocity data for supersonic jet of N_2 with 0.5% NO

- Eliminates need for particulate seeding
- Suitable for subsonic to hypersonic velocity measurements
- Potential for single-shot measurements of two velocity components
- Technique applicable to other molecular species, including OH, O_2 , Na and Cu



Comparison between measured and theoretical velocity components

Figure 10. New Broadband Laser Concept Enables Time-Resolved Velocity Field Measurements.

4.3 Future Work

During the next three years of the program we plan to continue the activities discussed above and to initiate new work in selected areas, as described in detail in our renewal proposal. This work includes:

- Complete assembly and characterization of the shock tunnel and plasma-heated supersonic flow facilities.
- Perform PLIF imaging of NO, O₂ and OH using single-laser PLIF in the shock tunnel, plasma-heated facility, and supersonic mixing layer facility.
- Continue research to develop PLIF schemes for imaging velocity and temperature using pulsed tunable dye lasers and pulsed tunable excimer lasers.
- Initiate research to extend PLIF to multiple-laser, multiple-camera concepts for simultaneous imaging of multiple parameters (species, temperature and velocity) and of single parameters in multiple planes.

5.0 COMPUTER SIMULATION AND ANALYSIS

5.1 Objectives

The objective of this portion of the program is to use numerical solutions of the governing equations to provide insight into the important physics controlling mixing and chemical reaction in high-speed flows. Two basic flows are being considered:

1. *Compressible mixing layer.* The purpose of this work is to develop understanding of the large-scale structure and macroscopic mixing in compressible mixing layers. Linearized stability analysis and accurate direct numerical simulations are the tools employed.
2. *Homogeneous compressible turbulence.* The purpose of this work is to develop understanding of the small-scale structure and microscopic mixing in compressible shear flows. The principal flow under study is homogeneous turbulence subjected to a uniform mean shear and uniform mean scalar gradient, and the primary tool is accurate direct numerical simulations.

5.2 Status of the Research

5.2.1 Linearized stability analysis for compressible mixing layers

Linearized stability calculations were carried out as the first step in the mixing layer program. The objective was to determine the most rapidly amplified modes in compressible mixing layers, for use in guiding subsequent direct numerical simulations.

The inviscid linearized equations were solved using both a direct and a shooting method. The shooting method was shown to be superior for weakly amplified waves at high Mach number and was subsequently used in all the calculations. The numerical methods were checked by running the code at low Mach numbers and comparing with published data. Calculations were performed for a variety of mixing layers with differing density and velocity ratios. These revealed the remarkable result that *linear theory can be used to predict mixing layer growth rates!* In each case where data are available, it was found that the spatial amplification rate of the most-amplified linear instability wave (2-D or 3-D) is proportional to the observed growth rate (spreading angle) of the developed shear layer. The proportionality factor depends upon the shear layer thickness parameter; for example, the vorticity thickness in the subsonic variable-density experiments of Brown and Roshko (1974) is 0.45 times the spatial amplification rate, while the factor for Bogdanoff's (1984) density profile thickness in supersonic shear layers is 0.6. The *ratio* of the growth rate at a Mach number greater than zero to that at Mach zero is given directly by the linearized analysis. A

similar result was observed for the velocity ratio effect in uniform density flows by Monkewitz and Huerre [1982]. For more details see paper 14 by Sandham and Reynolds listed in Section 6.0.

Another important finding from the stability analysis is that the most amplified wave is a 2-D wave only at low convective Mach numbers. Above a convective Mach number of 0.6, the most amplified wave is oblique, and the obliquity increases with increasing Mach number. The angle, θ , between the wave normal and the streamwise direction above $M_c = 0.6$ is approximately given by $M_c \cos \theta = 0.6$. The dominance of oblique waves at high Mach numbers suggests that the structure of the fully-developed turbulent mixing layer is also strongly three-dimensional.

Figure 11 shows the amplification rate predicted by linear stability theory as a function of the *convective Mach number*, M_c , proposed by Papamoschou and Roshko (1986) as a correlating parameter for shear layer growth rate. The three curves show three different methods of attaining high M_c . The third curve (dash-dot) corresponds to the experimental conditions described in Section 3.2.2 and may be considered a prediction of the experimental growth rate. The collapse of these three curves at low M_c confirms the importance of M_c in correlating experiments at low and moderate M_c . However, the M_c concept is based on a two-dimensional view of mixing layer structure. Considering this fact, and noting that the curves begin to diverge above $M_c = 0.6$, it appears that M_c may not collapse experimental data at high M_c .

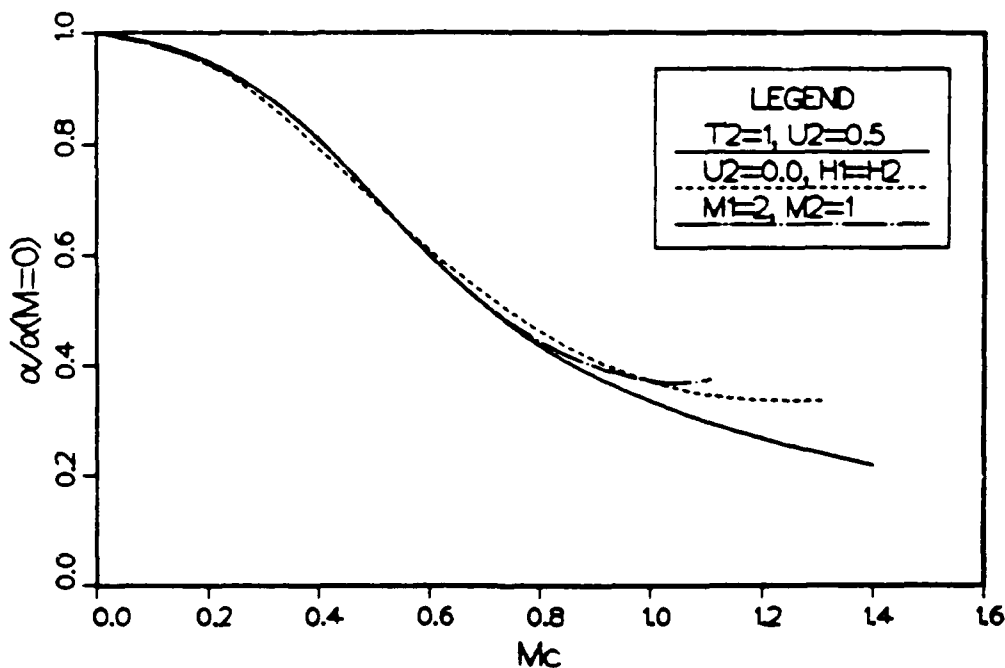


Fig. 11. Growth rate vs. convective Mach number from linearized stability analysis.

5.2.2 Mixing layer simulations

We began this work using shock-capturing methods of the TVD variety. Two-dimensional computations showed that the mixing layer grows slowly as the Mach number is increased, and the spanwise vortices become elongated in the streamwise direction by the action of the baroclinic torque; at high Mach numbers ($M_c > 0.7$) weak embedded shock waves were found. The TVD and MacCormack methods needed a large number of grid points to resolve the growth of the flow instability adequately. Therefore, this approach has been abandoned in favor of a more accurate approach.

We have adopted a new method developed at NASA/Ames for time-developing compressible mixing layers, for which calculations can be fast and accurate, allowing study of three-dimensional issues in depth. This method permits use of Fourier representations in the streamwise and cross-stream directions; a 6th-order modified Pade scheme is used in the mean-gradient direction, along with a mapping that emulates infinite free-stream. The code is explicit, with time advance by a third-order compact-storage Runge-Kutta scheme, and is implemented on the Cray X-MP 4/8 at NASA-Ames.

The new code was checked against the old for the case of two-dimensional flow. The same effects of the dilatation and baroclinic terms on vorticity transport were found, leading to elongated vortices. The same shock-wave structure at high Mach numbers is observed *in two-dimensional flows* with the new code.

As expected, the flow structure is quite different in three-dimensional simulations. A series of simulations have been performed at increasing Mach numbers, starting in each case with a superposition of a mean profile, the most amplified two-dimensional wave, and a pair of equal and opposite most-amplified three-dimensional waves. The flow structure is found to depend strongly on Mach number.

At low Mach number ($M_c = 0.4$), the main transverse structure develops from the two-dimensional instability, and the oblique waves lead to the Pierrehumbert & Widnall (1982) instability of the vortex cores and the development of streamwise vortices in the braids. At intermediate Mach number ($M_c = 0.8$), the two-dimensional and the oblique waves are approximately equally amplified, and the developed structure is strongly three-dimensional.

At high M_c , essentially for any $M_c > 1$, the oblique waves are dominant and grow many times faster than the two-dimensional wave in both the linear and non-linear regimes. The resulting structure is very three-dimensional, consisting of very oblique (nearly streamwise) vorticity, which alternates in sign in both the streamwise and spanwise directions. Eddy shocklets have *not* been found in any of these simulations, suggesting that

shocks found in two-dimensional simulations may be relieved by three-dimensionality.

Figures 12 and 13 show some results for a case at $M_c = 0.8$, similar to that of planned experiments. At higher Mach numbers we expect a similar but more oblique structure. Figure 12 shows various cuts of the scalar field: the horizontal cut in the upper-right corner is through the midplane of the layer, and the other cuts are defined there. Note the strong three-dimensionality of the flow. Cuts such as C-C and D-D plane may be deceiving, as they appear to show two-dimensional structures similar to that found at low M_c , even though the entire field is highly three-dimensional. This work has shown the importance of horizontal cuts for visualization in the experiments. Figure 13 shows the region of low pressure (vortex cores); note that the primary rollers are strongly oblique, and that they are connected by obliquely-inclined braid-like vortices. More details can be found in paper 13 by Sandham and Reynolds listed in Section 6.0.

5.2.3 Compressible isotropic turbulence

This work examines decaying compressible isotropic turbulence and compressible homogeneous shear flow. A passive scalar with a mean scalar gradient is included so that mixing may be studied. These simulations are designed to provide physical insight on the behavior of small-scale structures such as occur in the cores of the vortices in a supersonic mixing layer, and to guide the phenomenological modeling of this turbulence.

Direct simulations of decaying compressible isotropic turbulence have been performed using a highly-accurate pseudo-spectral method. Some important insights have been obtained from this work, and these are summarized below.

The first simulations performed were at relatively low rms Mach numbers $M \leq 0.3$ (Blaisdell *et al.*, paper 12 listed in Section 6.0). It was found that the presence of compressibility effects depends strongly on the initial conditions. If the initial velocity field is nearly divergence-free and the density fluctuations are weak, then the flow remains nearly incompressible; only small acoustic fluctuations are observed and the compressible terms in the averaged equations are negligible. On the other hand, if the initial conditions include large velocity divergences or density perturbations, then a strong acoustic mode will develop; in this case the compressible terms in the averaged equations are significant.

Simulations at higher rms Mach numbers where the interaction between the fluctuating vorticity and the acoustics would be stronger were attempted but it was found that the spatial resolution of the simulations was inadequate. In a direct simulation of turbulence there is a

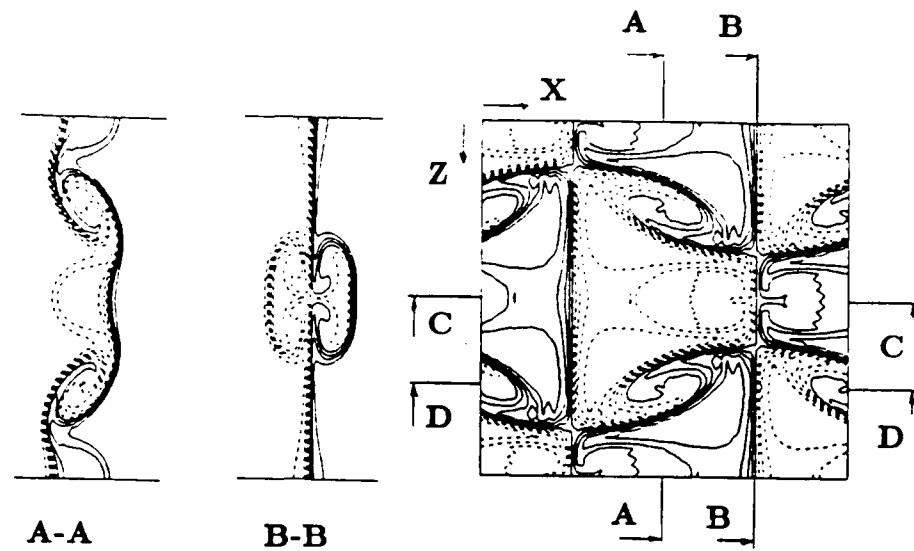


Fig. 12. Scalar contours for various sections through the simulated mixing layer at $M_c = 0.8$. The upper-right section is a cut through the midplane of the layer.

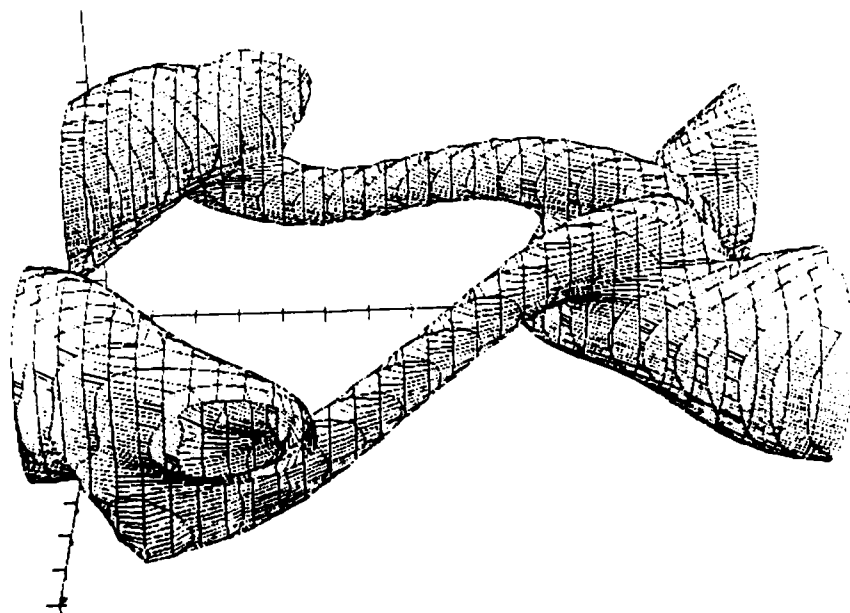


Fig. 13. Low-pressure surface in the simulated mixing layer at $M_c = 0.8$. Note the strongly oblique nature of the primary large-scale vortices.

trade-off between good spatial resolution and the number of eddies available for sampling within the computational domain. Future simulations are planned in which the sample size requirement is relaxed in order to improve the resolution.

The transport of a passive scalar in compressible isotropic turbulence was studied in some detail. The simulations include two passive scalars – one with and one without a mean scalar gradient. The scalar field that has a mean scalar gradient has initial conditions with no fluctuations. The turbulence acts on the mean scalar gradient to create a scalar flux which develops in time as shown in Figure 14.

Two incompressible turbulence models for the passive scalar flux were examined in order to establish baseline models that could be modified for compressibility effects. The incompressible models were formulated for the compressible problem by using Favre averaging. The first model is that of Rogers, Mansour and Reynolds (1988). It is an algebraic model which was developed using incompressible shear flow simulations. The modeled scalar flux is compared to direct simulation results in Figure 15 for a case that has negligible compressibility effects. An assumption made by the model is that the turbulence and the scalar fluctuations are in equilibrium which is not true during the early portion of the simulation. The model does predict the correct trend later in the simulation; however, the magnitude is off. The single model coefficient was set by matching incompressible shear flow results. By matching this coefficient to the current results, a better baseline model for compressible isotropic turbulence can be established.

The second model examined is the second-order closure model of Shih and Lumley (1986). It is an ordinary differential equation model involving a system of five equations. The model was developed for isotropic turbulence and agrees well with experimental results; however, the model does not agree well with the direct simulation results. This discrepancy has been shown to be due to a Reynolds number dependence that is not accounted for in the model coefficients which becomes important at the low Reynolds numbers of the simulation.

An interesting result which may prove useful in modeling passive scalar transport in compressible turbulence comes from looking at a decomposition of the velocity field used by Moyal (1951). The velocity field can be decomposed into a solenoidal part, u_i^s , and a dilatational part, u_i^d , where

$$\nabla \cdot \underline{u}^s = 0 \quad \text{and} \quad \nabla \times \underline{u}^d = 0 \quad .$$

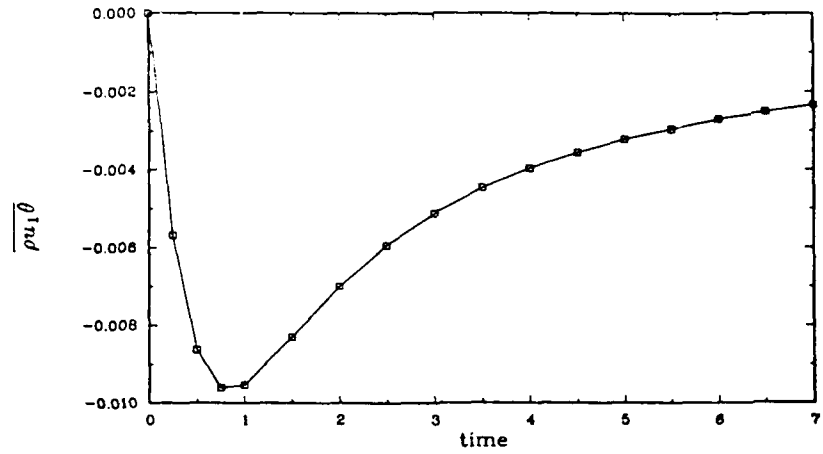


Fig. 14. Scalar flux history in the simulation of decaying isotropic turbulence.

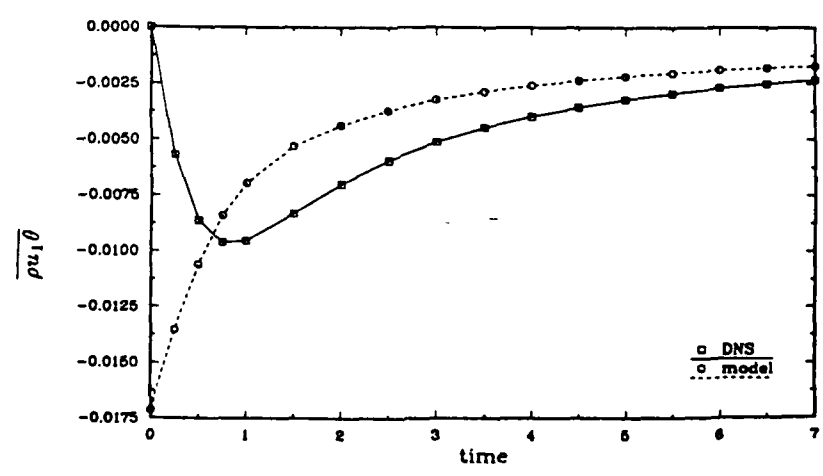


Fig. 15. Comparison of the scalar flux with the simple model of Rogers, Mansour, and Reynolds.

The solenoidal velocity field is associated with the vorticity and the dilatational velocity field is associated with volumetric compressions and expansions. One can form decomposed scalar fluxes as follows

$$\overline{\rho u_i^s \theta} \quad \text{and} \quad \overline{\rho u_i^d \theta}.$$

The full scalar flux and the decomposed scalar fluxes are shown in Figure 16 for a case in which the dilatational velocity correlation $\overline{u_i^d u_i^d}$ is 10–15% of the solenoidal velocity correlation $\overline{u_i^s u_i^s}$. One sees that the dilatational scalar flux is essentially zero so that only the solenoidal velocity generates a scalar flux. Simulations in which $\overline{u_i^d u_i^d}$ is several times larger than $\overline{u_i^s u_i^s}$ show that the dilatational velocity and the scalar are correlated for only a short time which corresponds to a single acoustic period. The dilatational velocity is associated with the acoustics leading to the conclusion that a random acoustic field does not do any mixing. This will be important for modeling scalar transport in cases where the acoustic mode contains a significant fraction of the turbulent kinetic energy.

A spectral code capable of simulating homogeneous shear flow has been prepared and is now undergoing check-out. This code is restricted to a linear variation of the mean velocity and uniform mean temperature, for which a homogeneous turbulent state can be attained. In addition, the transport of a scalar, driven by a uniform mean scalar gradient, can be examined.

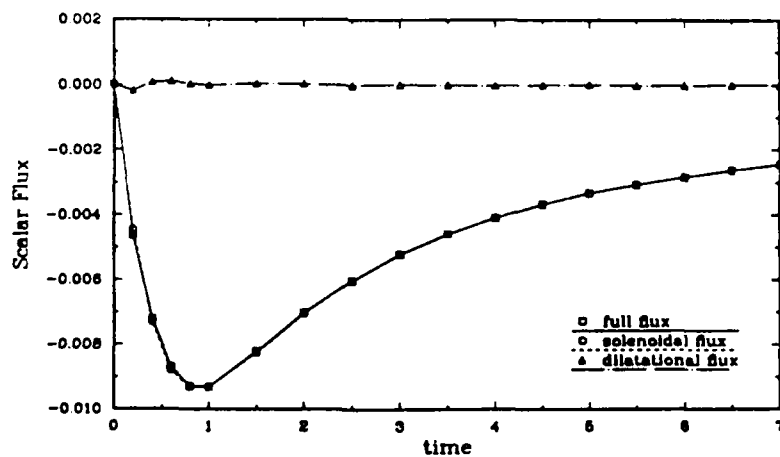


Fig. 16. History of the decomposed scalar fluxes for decaying isotropic compressible turbulence with a strong dilatational velocity component. Note that the dilatational part of the flow does not transport the scalar.

5.3 Future Work

During the next three years of the program we plan to continue the activities discussed above and to initiate new work in selected areas, as described in detail in our renewal proposal. This work includes:

- Initiate work on extension of linear stability analysis of compressible shear layers to include chemical reactions with heat release.
- Extend the simulation of compressible homogeneous turbulence to higher rms Mach numbers.
- Initiate work to formulate improved models for small-scale mixing in compressible flows.
- Incorporate fast-chemistry model into direct simulations of the 3-D mixing layer.
- Incorporate finite rate chemistry in direct numerical simulation codes.
- Compare results of the numerical simulations with experimental mixing layer data.

6.0 PUBLICATIONS AND PRESENTATIONS

During this program the following papers were written, published or presented:

1. Cohen, L. M., Lee, M. P., Paul, P. H. and Hanson, R. K. (1987), "Two-Dimensional Imaging Measurements in Supersonic Flows Using Laser-Induced Fluorescence of Oxygen," AIAA Paper 87-1527, AIAA 22nd Thermophysics Conference, Honolulu, HI.
2. Sandham, N. D. and Reynolds, W. C. (1987), "Some Inlet-Plane Effects on the Numerically Simulated Spatially-Developing, Two-Dimensional Mixing Layer," Turbulent Shear Flows 6, Toulouse, France.
3. Hanson, R. K. (1988), "Laser-Based Diagnostics for Gaseous Flows," invited paper presented at Workshop on Diagnostics for Ground-Based NASP Testing, West Palm Beach, FL.
4. Hanson, R. K. (1988), "Applications of PLIF Imaging to Supersonic Flows," invited presentation at Eleventh Sandia Cooperative Group Meeting, Livermore, CA.
5. Paul, P. H., Seitzman, J. J., Cohen, L. M., McMillin, B. K. and Hanson, R. K. (1988). "Planar Laser-Induced Fluorescence Imaging in Supersonic Flows," invited paper presented at CLEO '88, Anaheim, CA.
6. Hanson, R. K., Paul, P. H. and Seitzman, J. M. (1988), "Digital Fluorescence Imaging of Gaseous Flows," invited paper presented at Materials Research Society - Reno Meeting, Reno, NV.
7. Paul, P. H., Seitzman, J. M., Lee, M. P., McMillin, B. and Hanson, R. K. (1988). "Imaging of Supersonic Flows Using Planar Laser-Induced Fluorescence," poster paper presented at 22nd Symposium (International) on Combustion, Seattle, WA.
8. Hanson, R. (1988), "Advanced Diagnostic Techniques for Testing NASP Engine Modules," invited presentation at workshop on NASP/ETF program, Arnold AFB, TN.
9. Hanson, R. K. (1988), "Applications of PLIF Imaging to Supersonic Flows," invited paper presented at 54th National Aero-Space Symposium, NASA Langley Research Center, Hampton, VA.
10. Hanson, R. K. (1988), "Laser-Based Fluorescence Imaging of Gaseous Flows," invited paper presented at ICALEO '88, Santa Clara, CA.

11. Hiller, B. and Hanson, R. K. (1988), "Simultaneous Planar Measurements of Velocity and Pressure Fields in Gas Flows Using Laser-Induced Fluorescence," *Applied Optics* **27**, 33-48.
12. Blaisdell, G. A., Mansour, N. N, and Reynolds, W. C. (1988), "Numerical Simulation of Compressible Homogeneous Turbulence," *International Workshop of the Physics of Turbulent Compressible Mixing*, Princeton, NJ.
13. Sandham, N. D. and Reynolds, W. C. (1989), "The Growth of Oblique Waves in the Mixing Layer at High Mach Number," *Turbulent Shear Flows 7*, Stanford, CA.
14. Sandham, N. D. and Reynolds, W. C. (1989), "The Compressible Mixing Layer: Linear Theory and Direct Simulation," AIAA Paper 89-0371, AIAA 27th Aerospace Sciences Meeting, Reno, NV.
15. Hiller, B., Paul, P. H. and Hanson, R. K. (1989), "Image-Intensified Photodiode Array as a Fluorescence Detector in CW-Laser Experiments," *Review of Scientific Inst.*, in press.
16. Paul, P. H., Lee, M. P., McMillin, B. K., Cohen, L. M. and Hanson, R. K. (1989), "Planar Laser-Induced Fluorescence Imaging in Supersonic Flows," paper AIAA 89-0059, AIAA 27th Aerospace Sciences Meeting, Reno, NV.
17. Paul, P. H., Lee, M. P. and Hanson, R. K. (1989), "Molecular Velocity Imaging of Supersonic Flows Using Pulsed Planar Laser-Induced Fluorescence," *Optics Letters* **14**, 417-419 (1989).
18. McMillin, B. K., Paul, P. H., Lee, M. P., Seitzman, J. M., Palmer, J. L. and Hanson, R. K. (1989), "Planar Laser-Induced Fluorescence Imaging in a Shock Tube and Tunnel," reprint AIAA-89-2566 at 25th AIAA/ASME/ASCE/SAE Joint Propulsion Conference, Monterey, CA, July 10-12, 1989.
19. Paul, P. H., Seitzman, J. and Hanson, R. K. (1989), "Planar Laser-Induced Fluorescence Imaging in Reacting Supersonic Flows," reprint AIAA-89-2912 at 25th AIAA/ASME/ASCE/SAE Joint Propulsion Conference, Monterey, CA, July 10-12, 1989.
20. McMillin, B. K., Paul, P. H., Lee, M. P., and Hanson, R. K. (1989), "Planar Laser-Induced Fluorescence Imaging of Supersonic Flows in Vibrational Nonequilibrium," to be presented at ASME Winter 1989 Meeting, San Francisco, CA, Dec. 1989.

21. Lee, M. P., McMillin, B. K., Paul, P. H. and Hanson, R. K., "PLIF Imaging in Supersonic Flows," paper 89-40 at WSS/CI Fall Meeting, Livermore, CA, Oct. 23-24, 1989.
22. Clemens, N. T., Mungal, M. G., Berger, T. E. and Vandsburger, U., "Visualizations of a Compressible Turbulent Mixing Layer," Seventh Symposium on Turbulent Shear Flows, Stanford Univ., Aug. 1989.
23. Clemens, N. T., Mungal, M. G., Berger, T. E. and Vandsburger, U., "Observations of the Structure of a Compressible Mixing Layer," presented at the 42nd Annual Meeting of the American Physical Society/Division of Fluid Dynamics, Palo Alto, Nov. 1989.
24. Clemens, N. T., Mungal, M. G., Berger, T. E. and Vandsburger, U., "Visualizations of the Structure of the Turbulent Mixing Layer under Compressible Conditions," AIAA-90-0500, presented at the 29th Aerospace Sciences Meeting, Reno, Jan. 1990.
25. Miller, M. F., Bowman, C. T., Miller, J. A. and Kee, R. J., "A Model for Chemical Reaction in a Compressible Mixing Layer," Paper 89-110, Western States Section, The Combustion Institute, Oct. 1989.

7.0 PERSONNEL

Craig T. Bowman	Professor, Mechanical Engineering
Ronald K. Hanson	Professor, Mechanical Engineering
Mark Godfrey Mungal	Assistant Professor, Mechanical Engineering
William C. Reynolds	Professor, Mechanical Engineering
Phillip H. Paul	Senior Research Associate, Mechanical Engineering
Uri Vandsburger	Research Associate, Mechanical Engineering
Thomas Berger	Graduate Research Assistant, Mechanical Engineering
Gregory A. Blaisdell	Graduate Research Assistant, Mechanical Engineering
Noel T. Clemens	Graduate Research Assistant, Mechanical Engineering
Larry M. Cohen	Graduate Research Assistant, Mechanical Engineering
Michael P. Lee	Graduate Research Assistant, Mechanical Engineering
Michael F. Miller	Graduate Research Assistant, Mechanical Engineering
Neil D. Sandham	Graduate Research Assistant, Mechanical Engineering
Brian McMillin	Graduate Research Assistant, Mechanical Engineering

8.0 PROFESSIONAL INTERACTIONS

During the past three years, we have had numerous interactions with individuals at government, industrial and university laboratories involved with supersonic combustion, laser diagnostics and computational fluid dynamics.

In the area of supersonic combustion, we have established a working relationship with Cal Tech, the University of Illinois, NASA/Ames and NASA Langley Research Centers, and the Applied Physics Laboratory. We have had numerous visitors not only from these organizations, but also from companies involved in the National Aerospace Plane (NASP) project, including McDonnell-Douglas, General Electric, United Technologies, Boeing and Rocketdyne.

Our research on flowfield diagnostics has generated considerable interest in the aerodynamics and propulsion communities, particularly owing to the potential utility of the methods for research related to the NASP. The level of interest shown suggests that this research project has potential for significant impact on the national research effort for NASP.

The computations are being carried out in collaboration with the NASA/Ames Research Center, which is providing computer time on Ames supercomputers. Ames' experts in numerical analysis for turbulence and compressible flows have provided important consultation in the development of the programs. This work has been integrated into the supersonic simulation effort of the new Stanford/Ames Center for Turbulence Research, which has identified the simulation of compressible turbulence as a key thrust area.

9.0 REFERENCES

- Andresen, P. (1988), private communication.
- Bogdanoff, D. W. (1983), "Compressibility Effects in Turbulent Shear Layers," *AIAA J.* **21**, 926.
- Bogdanoff, D. W. (1984), "Interferometric Measurement of Heterogeneous Shear-Layer Spreading Rates," *AIAA Journal* **22**, 1550.
- Broadwell, J. E. and Breidenthal, R. (1982), "A Simple Model of Mixing and Chemical Reaction in a Turbulent Shear Layer," *J. Fluid Mech.* **125**, 397.
- Broadwell, J. E. and Mungal, M. G. (1988), "Molecular Mixing and Chemical Reactions in Turbulent Shear Layers," *Twenty-Second Symp. (Int'l) on Combustion*, The Combustion Institute, 579.
- Brown, G. L. and Roshko, A. (1974), "On Density Effects and Large Structure in Turbulent Mixing Layers," *J. Fluid Mech.* **64**, 775.
- Burrows, M. C., and Kurkov, A. P. (1973), "Analytical and Experimental Study of Supersonic Combustion of Hydrogen in a Vitiated Airstream, NASA-TM-X-2828.
- Monkewitz, P. A. and Huerre, P. (1982), "Influence of the Velocity Ratio on the Spatial Instability of Mixing Layers," *Phys. Fluids* **25**, 1137.
- Moyal, J. E. (1951), "The Spectra of Turbulence in a Compressible Fluid: Eddy Turbulence and Random Noise," *Proc. Camb. Phil. Soc.* **48**, 329.
- Papamoschou, D. and Roshko, A. (1986), "Observations of Supersonic Free Shear Layers," *AIAA Paper 86-0162*, 24th AIAA Aerospace Sciences Meeting, Reno, NV.
- Papamoschou, D. (1989), "Structure of the Compressible Turbulent Mixing Layer", *AIAA Paper 89-0126*, 27th AIAA Aerospace Sciences Meeting, Reno, NV.
- Pierrehumbert, R. T. and Widnall, S. E. (1982), "The Two- and Three-Dimensional Instabilities of a Spatially Periodic Shear Layer," *J. Fluid Mech.* **114**, 59.
- Rogers, M. M., Mansour, N. N. and Reynolds, W. C. (1989), "An Algebraic Model for the Turbulent Flux of a Passive Scalar," *J. Fluid Mech.*, to appear.
- Shih, T.-H. and Lumley, J. L. (1986), "Influence of Timescale Ratio on Scalar Flux Relaxation: Modelling Sivirat & Warhaft's Homogeneous Passive Scalar Fluctuations," *J. Fluid Mech.* **162**, 211.